J|A|C|S
ARTICLES
Published on Web 08/23/2002

The Initial Steps in the Hydration of Unsolvated Peptides: Water Molecule Adsorption on Alanine-Based Helices and Globules

Motoya Kohtani and Martin F. Jarrold*,†

Contribution from the Department of Chemistry, Northwestern University, 2145 Sheridan Road, Evanston, Illinois 60208

Received December 27, 2001

Abstract: Equilibrium constants for the adsorption of the first water molecule onto a variety of unsolvated alanine-based peptides have been measured and ΔH° and ΔS° have been determined. The studies were designed to examine the effects of conformation, charge, and composition on the propensity for peptides to bind water. In general, water adsorption occurs significantly more readily on the globular peptides than on helical ones: several of the singly charged helical peptides were not observed to adsorb a water molecule even at −50 °C. These results place a limit on the free energy change for interaction between a water molecule and the helical peptide group. Molecular dynamics simulations reproduce most of the main features of the results. The ability to establish a network of hydrogen bonds to several different hydrogen-bonding partners emerges as a critical factor for strong binding of the water molecule. Whether the charge site is involved in water adsorption depends on how well it is shielded. Peptides containing a protonated histidine bind water much more strongly that those containing a protonated lysine because the delocalized charge on histidine is difficult to shield. The entropy change for adsorption of the first water molecule is correlated with the enthalpy change.

Introduction

Unlike other heteropolymers, which tend to either dissolve readily or be insoluble in water, proteins have a delicate balance between their hydrophobic and hydrophilic interactions.[1−5] Small changes can often have drastic consequences; for example, many proteins precipitate out of solution when they denature. Another example where conformation has a dramatic effect on solubility is provided by the amyloid diseases.[6,7] This diverse group of conditions is characterized by conversion of soluble protein into insoluble amyloid fibrils, which deposit in various tissues throughout the body. This change in solubility is brought about by a conformational change.

In addition to the conformation affecting the solubility, the solvent exerts a strong influence on the conformations of peptides and proteins in solution. The three-dimensional structures are determined by a complex interplay between intramolecular interactions and interactions between the protein and the solvent. A variety of methods have been used to study the hydration of proteins and peptides, including microcalorimetry,[8,9] neutron scattering,[10] NMR,[11] and molecular dynamics (MD) simulations.[12−17] While it is straightforward to examine the behavior of individual water molecules by MD, the experimental methods mentioned above usually provide information that is averaged over many water molecules. However, with recent experimental advances, it is possible to study sparsely hydrated biological molecules in the gas phase and obtain information as a function of the number of adsorbed water molecules.[18] Several different approaches have been employed, including studies of partially desolvated peptides generated by electrospray,[19−21] studies of the rehydration of unsolvated peptides and proteins,[22−25] and spectroscopic studies of jet-cooled hydrated clusters of small biomolecules.[26−29]

* Address correspondence to this author. E-mail: mfj@indiana.edu.
† Present address: Chemistry Department, Indiana University, 800 E. Kirkwood Ave., Bloomington, IN 47405-7102.

(1) Kauzmann, W. *Adv. Protein Chem.* **1959**, *14*, 1−63.
(2) Kuntz, I. D.; Kauzmann, W. *Adv. Protein Chem.* **1974**, *28*, 239−345.
(3) Richards, F. M. *Annu. Rev. Biophys. Bioeng.* **1977**, *6*, 151−176.
(4) Rupley, J. A.; Gratton, E.; Careri, G. *Trends Biochem. Sci.* **1983**, *8*, 18−22.
(5) Dill, K. A. *Biochemistry* **1985**, *24*, 1501−1509.
(6) Sipe, J. D.; Cohen, A. S. *J. Struct. Biol.* **2000**, *130*, 88−98.
(7) Dobson, C. M. *Philos. Trans. R. Soc. London B* **2001**, *356*, 133−145.
(8) Yang, P. H.; Rupley, J. A. *Biochemistry* **1979**, *18*, 2654−2661.
(9) Doster, W.; Bachleitner, A.; Dunau, R.; Heibl, M.; Lüscher, E. *Biophys. J.* **1986**, *50*, 213-219.
(10) Teeter, M. M. *Annu. Rev. Biophys. Chem.* **1991**, *20*, 577−600.
(11) Ötting, G.; Liepinsh, E.; Wüthrich, K. *Science* **1991**, *254*, 974−980.
(12) Steinbach, P. J.; Brooks, B. R. *Proc. Natl. Acad. Sci. U.S.A.* **1993**, *90*, 9135−9139.
(13) Doruker, P.; Bahar, I. *Biophys. J.* **1997**, *72*, 2445−2456.
(14) Garcia, A. E.; Hummer, G.; Soumpasis, D. M. *Proteins* **1997**, *27*, 471−480.
(15) Tirado-Rives, J.; Maxwell, D. S.; Jorgensen, W. L. *J. Am. Chem. Soc.* **1993**, *115*, 11590−11593.
(16) Gerstein, M.; Lyndon-Bell, R. M. *J. Phys. Chem.* **1993**, *97*, 2991−2999.
(17) Mao, Y.; Ratner, M. A.; Jarrold, M. F. *J. Am. Chem. Soc.* **2001**, *123*, 6503−6507.
(18) Jarrold, M. F. *Annu. Rev. Phys. Chem.* **2000**, *51*, 179−207.
(19) Chowdhury, S. K.; Katta, V.; Chait, B. T. *Rapid Commun. Mass Spectrom.* **1990**, *4*, 81−87.
(20) Rodriguez-Cruz, S. E.; Klassen, J. S.; Williams, E. R. *J. Am. Soc. Mass Spectrom.* **1997**, 565−568.
(21) Lee, S. W.; Freivogel, P.; Schindler, T.; Beauchamp, J. L. *J. Am. Chem. Soc.* **1998**, *120*, 11758−11765.
(22) Klassen, J. S.; Blades, A. T.; Kebarle, P. *J. Phys. Chem.* **1995**, *99*, 15509−15517.

10.1021/ja012755r CCC: $22.00

In this article, we report studies of the rehydration of alanine-based peptides. The enthalpy and entropy changes associated with the addition of the first water molecule to the peptides were obtained from gas-phase ion equilibrium measurements. Ion equilibrium measurements have been used for many years to study the interactions between water and a variety of small molecules.[30−36] While this approach has been used to examine the rehydration of individual amino acids and small polypeptides,[22,37] as well as proteins,[24] to our knowledge this is the first time these experiments have been performed on polypeptides that are large enough to adopt secondary structure. The alanine-based peptides studied here were selected because previous work has shown that the conformations of the protonated peptides can be switched between helical and globular (a compact random-looking structure) through the interaction of the charge with the helix dipole.[38,39] Furthermore, the study of the hydration of alanine-based peptides is simplified by alanine's hydrophobic side chain; more hydrophilic residues may become involved in complicated side-chain interactions, which renders analysis more difficult. Our measurements show that the globular Ac-KA_{20}+H^+ (Ac = acetyl, A = alanine, and K = lysine) adsorbs water far more strongly than α-helical Ac-A_{20}K+H^+. However, we were not able to obtain quantitative information about the different hydration tendencies of the helix and the globule because we were unable to observe significant water absorption on the helix under any experimental conditions. Molecular dynamics (MD) simulations indicate that a network of hydrogen bonds binds the water to the globular Ac-KA_{20}+H^+, while no such network exists for the counterpart. We have studied the hydration of the shorter analogues, Ac-A_{15}K+H^+ and Ac-A_{15}K+H^+, to determine whether peptide length plays any role. We have also examined the hydration of doubly charged Ac-A_{15}K+$2H^+$, Ac-KA_{20}+$2H^+$, and Ac-A_{20}K+$2H^+$. As might be anticipated, the doubly charged peptides bind water slightly more strongly. Finally, we have examined some peptides, such as Ac-A_{15}HGH-NH_2+$2H^+$ (H = histidine and G = glycine) and Ac-A_{15}H, that were specifically designed to bind water strongly.

Experimental Section

All experimental data were obtained using a variable-temperature, injected-ion drift tube apparatus that has been described in detail elsewhere.[40] Briefly, the ions are produced by an electrospray source and desolvated in a heated capillary. The ions are then injected into a 30.5 cm long drift tube. The drift tube is made up of four sections which can be cooled by liquid nitrogen; the temperature of each section is regulated to better than ±0.5 K by means of microprocessor-based temperature controllers. The drift tube contains a series of guard rings to ensure a uniform electric field along its length, and it is filled with He buffer gas to a pressure of around 4 Torr. After traveling across the drift tube under the influence of a weak electric field, some of the ions exit through a small aperture. These ions are focused into a quadrupole mass spectrometer, and after being mass analyzed, they are detected by an off-axis collision dynode and dual microchannel plates. In the present studies, two different types of measurement were performed: drift time and equilibrium measurements.

Drift times are obtained by using an electrostatic shutter to admit a short (50−100 μs) pulse of ions into the drift tube and recording the ions' arrival time distribution at the detector. The arrival time distribution is then converted into a drift time distribution by accounting for flight time outside of the drift tube. The drift times are converted into collision cross sections using[41]

$$\Omega_{\mathrm{avg}}^{(1,1)} = \frac{(18\pi)^{1/2}}{16}\left[\frac{1}{m}+\frac{1}{m_{\mathrm{b}}}\right]^{1/2}\frac{ze}{(k_{\mathrm{B}}T)^{1/2}}\frac{t_{\mathrm{D}}E}{L}\frac{1}{\rho} \qquad (1)$$

where m is the mass of the peptide ion, m_{b} is the mass of the buffer gas, E is the drift field, L is the length of the drift tube, and ρ is the buffer gas number density.

Equilibrium measurements were performed by admitting a known partial pressure of water vapor in the drift tube and recording the intensity of the reactants and products in the mass spectrum. The water vapor pressure was regulated with a leak valve, and the measured pressure was corrected to account for the effect of the buffer gas flow. The corrected water vapor partial pressures employed were typically in the 1−7 mTorr range, with around 4 Torr of helium buffer gas. It is important that these measurements be performed under low-field conditions, where the collisional heating caused by the drift field is negligible. The critical quantity for ascertaining low-field conditions is E/p (drift field/total pressure).[41] Most of our experimental data were obtained with a drift voltage of 280 V, which gives an $E/p \approx 2.3$ V/cm-Torr for singly charged ions. Some measurements were also done with a drift voltage of 180 V ($E/p \approx 1.5$ V/cm-Torr), and these were not significantly different from measurements performed with a drift voltage of 280 V. Klassen et al. have conducted similar gas-phase equilibrium measurements at 2 V/cm-Torr.[22] Keesee et al. have reported equilibria with E/p near 15 V/cm-Torr.[42] A simple estimate of an effective temperature increase due to collisional heating by the drift field can be obtained from[43]

$$\delta T_{\mathrm{eff}} = \frac{m_{\mathrm{B}}\, v_{\mathrm{d}}^2}{2k_{\mathrm{B}}} \qquad (2)$$

where v_{D} is the drift velocity. With the conditions employed here, the estimated effective temperature increase is well below 1 K. A number of steps were taken to ensure that equilibrium was, in fact, established. First, as noted above, measurements performed with drift voltages of 180 and 280 V gave identical results for all the peptides discussed here. Second, drift time distributions of the unsolvated and hydrated ions are virtually identical, which is expected if an equilibrium is established. However, for the relatively large ions studied here, this is an insensitive test for equilibrium because addition of a single water molecule does not cause a significant change in the mobility. For the Ac-A_{15}H+H^+ peptide, the drift time distributions for the unsolvated

(23) Woenckhaus, J.; Mao, Y.; Jarrold, M. F. *J. Phys. Chem. B* **1997**, *101*, 847−851.
(24) Woenckhaus, J.; Hudgins, R. R.; Jarrold, M. F. *J. Am. Chem. Soc.* **1997**, *119*, 9586−9587.
(25) Fye, J. L.; Woenckhaus, J.; Jarrold, M. F. *J. Am. Chem. Soc.* **1998**, *120*, 1327−1328.
(26) Zwier, T. S. *J. Phys. Chem. A* **2001**, *105*, 8827−8839.
(27) Mons, M.; Dimicoli, I.; Tardivel, B.; Piuzzi, F.; Robertson, E. G.; Simons, J. P. *J. Phys. Chem. A* **2001**, *105*, 969−973.
(28) Robertson, E. G.; Simons, J. P. *Phys. Chem. Chem. Phys.* **2001**, *3*, 1−18.
(29) Robertson, E. G.; Hockridge, M. R.; Jelfs, P. D.; Simons, J. P. *J. Phys. Chem. A* **2000**, *104*, 11714−11724.
(30) For a recent review, see: Kebarle, P. *Int. J. Mass Spectrom.* **2000**, *200*, 313−330.
(31) Lau, Y. K.; Kebarle, P. *Can. J. Chem.* **1981**, *59*, 151−155.
(32) Meot-Ner (Mautner), M. *J. Am. Chem. Soc.* **1984**, *106*, 1265−1272.
(33) Meot-Ner (Mautner), M.; Speller, C. V. *J. Phys. Chem.* **1986**, *90*, 6616−6626.
(34) Meot-Ner (Mautner), M. *J. Am. Chem. Soc.* **1988**, *110*, 3071−3075.
(35) Meot-Ner (Mautner), M. *J. Am. Chem. Soc.* **1988**, *110*, 3075−3080.
(36) Blades, A. T.; Klassen, J. S.; Kebarle, P. *J. Am. Chem. Soc.* **1996**, *118*, 12437−12442.
(37) Meot-Ner (Mautner), M. *J. Am. Chem. Soc.* **1984**, *106*, 278−283.
(38) Hudgins, R. R.; Ratner, M. A.; Jarrold, M. F. *J. Am. Chem. Soc.* **1998**, *120*, 12974−12975.
(39) Hudgins, R. R.; Jarrold, M. F. *J. Am. Chem. Soc.* **1999**, *121*, 3494−3501.
(40) Kinnear, B. S.; Hartings, M. R.; Jarrold, M. F. *J. Am. Chem. Soc.* **2001**, *123*, 5660−5667.
(41) Mason E. A.; McDaniel E. W. *Transport Properties of Ions in Gases*; Wiley: New York, 1988.
(42) Keesee, R. G.; Lee, N.; Castleman, A. W., Jr. *J. Am. Chem. Soc.* **1979**, *101*, 2599−2604.
(43) Wannier, G. H. *Phys. Rev.* **1951**, *83*, 281−289.

peptide and for the adduct with a single water molecule are significantly different at low temperature. As we discuss further below, there appear to be two Ac-$A_{15}H+H^+$ conformations at low temperature with slightly different water affinities.

Equilibrium constants were obtained from

$$K = \frac{I_{\text{peptide}-\text{water}}}{I_{\text{peptide}} P_{\text{water}}} \quad (3)$$

where I_{peptide} and $I_{\text{peptide}-\text{water}}$ are the intensities in the mass spectrum of the unsolvated peptide ion and the peptide ion with a single water molecule attached, and P_{water} is the partial pressure of water in the drift tube in atmospheres. The intensities were obtained by integrating the peaks in the mass spectrum using Origin 5.0. As a test of our procedures, we examined the hydration of G_2+H^+, which has previously been studied by Klassen et al.[22] at 293 K. At the same temperature, we found a good linear relationship between the $I_{\text{peptide}-\text{water}}/I_{\text{peptide}}$ intensity ratio and the water partial pressure. The standard Gibbs free energy change ($\Delta G°$) for addition of the first water to G_2+H^+ at 293 K was found to be -35.1 kJ mol^{-1}, in good agreement with the -36.8 kJ mol^{-1} value reported by Klassen et al.[22] Our value for $\Delta G°$ for addition of the second water to G_2+H^+ is -25.1 kJ mol^{-1}, in good agreement with their value of -25.9 kJ mol^{-1}. Klassen et al. reported that their $\Delta G°$ values were generally more negative than accepted values by 0.4−4.0 kJ mol^{-1}. They suggested that this might be due to condensation of water onto the ions just outside the sampling orifice. On the other hand, our values of $\Delta G°$ might be slightly less negative than the values reported by Klassen et al. because of collisional activation in the same region, causing loss of water from the hydrated ions. For G_2+H^+, the singly hydrated ion is by far the most abundant ion in the mass spectrum, which means that the $I_{\text{peptide}-\text{water}}/I_{\text{peptide}}$ intensity ratio is particularly sensitive to collisional activation. The larger peptides studied here have a substantially lower affinity for water than G_2+H^+, and so collisional activation is not expected to be a significant source of error.

Doubly charged dimers and other higher order multimers are a potential source of error because they have the same m/z ratio as the singly charged peptide, and thus they are hidden in a low resolution mass spectrum (in the absence of water).[44] The presence of dimers and other multimers can usually be discerned from the drift time distributions. The dimers and other multimers were largely eliminated by raising the injection energy (the potential difference between the exit of the electrospray source and the entrance of the drift tube) to 500−600 eV, or by raising the temperature of the heated capillary (by increasing the temperature of the metal block in which the capillary is mounted from its normal operating temperature of around 100 °C to 120−150 °C). In some cases, such as the Ac-$KA_{20}+H^+$ peptide, a small amount of dimer persisted, even with the increased injection energy and raised capillary temperature.

Peptide Synthesis

All peptides with the exception of G_2 were synthesized using *FastMoc* chemistry on the Applied Biosystems model 433A peptide synthesizer. After cleavage with a cocktail of 95% trifluoroacetic acid (TFA) and 5% water, peptides were precipitated, centrifuged, and then lyophilized. G_2 at 99+% was obtained from ACROS Organic. For all but G_2, the electrospray solution consisted of 2 mg of peptide in 1.0 mL of TFA and 0.1 mL of water. The optimum signal for G_2 was found to result from a solution of 1 mg in 10 mL of methanol and 5 drops of glacial acetic acid.

Experimental Results

Equilibrium constants were measured at various temperatures, and van't Hoff plots (ln K against $1/T$) were obtained. An example is shown in Figure 1 for the Ac-$KA_{20}+H^+$ peptide. It is evident that the results generate a good straight line ($R^2 = 0.975$). The van't Hoff plots for all peptides studied here have $R^2 > 0.97$. The reproducibility of the equilibrium constants for Ac-$KA_{20}+H^+$ (shown in Figure 1) is not as good as those for the other peptides studied. This is attributed to a small amount of the dimer, $(AcKA_{20})_2+2H^+$, that survived in some of the experiments. The slope of the van't Hoff plot is $-\Delta H°/R$, while the intercept is $\Delta S°/R$. For addition of the first water molecule to $AcKA_{20}+H^+$, we obtain from Figure 1 that $\Delta H° = -47.0$ kJ mol^{-1} and $\Delta S° = -114$ J K^{-1} mol^{-1}. The results obtained from the van't Hoff plots are summarized in Table 1. The uncertainty estimates in the table are derived from the standard deviations of the slopes and intercepts of the van't Hoff plots of n points multiplied by the 95% confidence interval coefficients from the Student's t-distribution for $n-2$ degrees of freedom.[45] In the past, it has been found that equilibrium-based measurements from different groups usually agree to within 4 kJ mol^{-1} for $\Delta H°$ and to within 8 J K^{-1} mol^{-1} for $\Delta S°$.

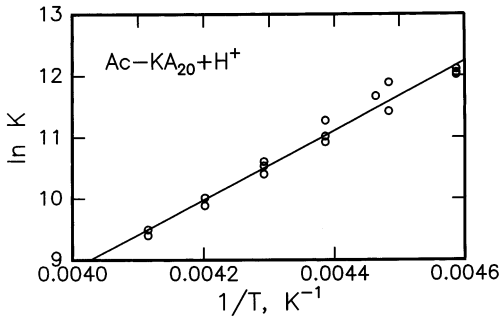

Figure 1. Van't Hoff plot (ln K against $1/T$) for the addition of the first water molecule to Ac-$KA_{20}+H^+$. The points are the measurements, and the line is a linear least-squares fit.

Ion mobility measurements and molecular dynamics simulations for $AcKA_{20}+H^+$ show that this peptide adopts a globular conformation in the gas phase.[38,39] On the other hand, $AcA_{20}K+H^+$, with the lysine at the C-terminus, is an α-helix. The difference in the conformation is attributed to the location of the lysine, which is expected to carry the charge. In $AcKA_{20}+H^+$, the protonated lysine side chain is at the N-terminus, where unfavorable interactions between the charge and the helix macrodipole disrupt helix formation, while in $AcA_{20}K+H^+$, the protonated lysine interacts favorably with the helix macrodipole and further stabilizes the helix by forming hydrogen bonds to the dangling CO groups at the C-terminus.[38,39] Despite examining a wide range of experimental conditions, we failed to observe any significant amount of water adsorption on the $AcA_{20}K+H^+$ helix. Figure 2 shows mass spectra recorded for globular $AcKA_{20}+H^+$ and helical $AcA_{20}K+H^+$ with around 5.9 mTorr H_2O in the drift tube and with a drift tube temperature near 224 K. While water adsorbs quite well onto the globular Ac-$KA_{20}+H^+$ peptide (a maximum of two water molecules were found to adsorb), the helical Ac-$A_{20}K+H^+$ shows no evidence of any adsorption. For most of the experiments, we kept the water vapor partial pressure in the drift tube below 8 mTorr in order to prevent water condensation on ions at the exit aperture and increased scattering from water molecules outside the drift tube. Some measurements

(44) Counterman, A. E.; Valentine, S. J.; Srebalus, C. A.; Henderson, S. C.; Hoagland, C. S.; Clemmer, D. E. *J. Am. Soc. Mass Spectrom.* **1998**, *9*, 743−759.

(45) Meot-Ner, M.; Sieck, L. W.; Liebman, J. F.; Scheiner, S. *J. Phys. Chem.* **1996**, *100*, 6445−6450.

Table 1. Experimental Values for $\Delta H°$, $\Delta S°$, and $\Delta G°$, and Values of $\Delta H°$ Deduced from the MD Simulations for Addition of the First Water Molecule to the Peptides Studied Here

		experimental values				
				$\Delta G°$, kJ mol^{-1}		
peptide	structural assignment	$\Delta H°$, kJ mol^{-1}	$\Delta S°$, J K^{-1}mol^{-1}	243 K	293 K	calcd $\Delta H°$,[a] kJ mol^{-1}
Ac-KA_{20} + H^+	glob	−47.0(3.5)	−114(15)[b]	−19.3	−13.6	−52
Ac-$A_{20}K$ + H^+	helix			> −10[c]		−43
Ac-KA_{20} + $2H^+$	glob	−47.7(2.7)	−92(11)	−25.3	−20.7	−50
Ac-$A_{20}K$ + $2H^+$	helix	−40.6(1.9)	−87(8)	−19.5	−15.1	−49
Ac-KA_{15} + H^+	glob	−48.9(2.3)	−131(10)	−17.1	−10.5	−60
Ac-$A_{15}K$ + H^+	helix					−47
Ac-$A_{15}K$ + $2H^+$	helix	−47.6(2.4)	−114(10)	−19.9	−14.2	−54
Ac-A_{15}HGH-NH_2 + $2H^+$	helix	−59.9(4.7)	−162(19)	−20.5	−12.4	−51 (−71)[d]
Ac-$A_{15}H$ + H^+	helix	−62.7(3.0)	−187(13)	−17.3	−7.9	−53 (−61)[d]

[a] The calculated $\Delta H°$ is assumed to be given by the negative of the water-binding energy (the average potential energy with the water bound minus the average potential energy without a bound water molecule) [b] Uncertainty estimates, in parentheses, are derived from the standard deviations of the slopes and intercepts of the van't Hoff plots of n points multiplied by the 95% confidence interval coefficients from the Student's t-distribution for $n - 2$ degrees of freedom.[45] [c] Assuming it is possible to detect a product of 2% of the reactant at an H_2O partial pressure of 113 mTorr at 243 K (see text). [d] After manipulating the conformations of Ac-A_{15}HGH-NH_2+$2H^+$ and Ac-$A_{15}H$ + H^+ to find stronger binding sites (see text).

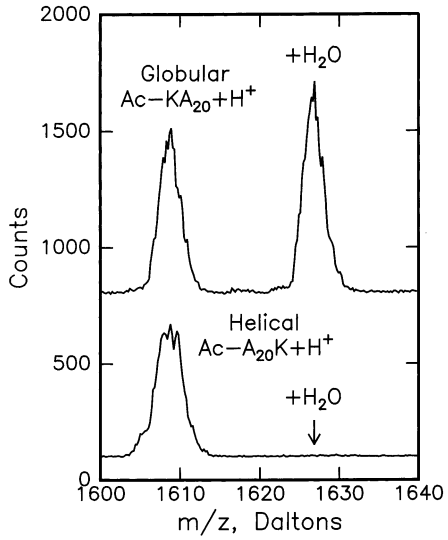

Figure 2. Mass spectra recorded for Ac-KA_{20}+H^+ and Ac-A_{20}K+H^+ with around 5.9 mTorr H_2O in the drift tube and with a drift tube temperature near 224 K. The spectrum for Ac-KA_{20}+H^+ is offset for clarity.

were performed for helical Ac-A_{20}K+H^+ with much higher water vapor pressure. Even with 113 mTorr water vapor partial pressure at 243 K, there was no sign of water adsorption. Assuming, conservatively, that it is possible to detect a product that is 2% of the reactant intensity, this places an upper limit of > -10 kJ mol^{-1} on the Gibbs free energy change for hydration of helical Ac-A_{20}K+H^+ at 243 K.

We examined the hydration of doubly charged Ac-KA_{20}+$2H^+$ and Ac-A_{20}K+$2H^+$ to determine how the extra charge affects the behavior. The conformations of these species were not determined prior to this work. Cross sections obtained for the Ac-KA_{20}+$2H^+$ and Ac-A_{20}K+$2H^+$ peptides from ion mobility measurements are shown in Table 2. Comparison with the cross sections for the singly charged analogues, Ac-KA_{20}+H^+ and Ac-A_{20}K+H^+, and with the results of molecular dynamics simulations (see below) indicates that the doubly charged peptides have the same types of comformations as the singly charged ones: Ac-KA_{20}+$2H^+$ is a compact globule and Ac-A_{20}K+$2H^+$ is helical.

Both Ac-KA_{20}+$2H^+$ and Ac-A_{20}K+$2H^+$ adsorb water more strongly than the singly charged analogues. Up to three water molecules adsorb on globular Ac-KA_{20}+$2H^+$, and measurable

Table 2. Measured and Calculated Collision Cross Sections and Structural Assignments for the Peptides Studied Here

	cross section, Å^2 [a]		structural
peptide	measured	calculated[b]	assignment
Ac--KA_{20}+H^+	332	335	glob
Ac-A_{20}K +H^+	381	380	helix
Ac-KA_{20}+$2H^+$	336	329	glob
Ac-A_{20}K +$2H^+$	377	361	helix
Ac-KA_{15}+H^+	274	279	glob
Ac-A_{15}K+H^+	308	303	helix
Ac-A_{15}K+$2H^+$	304	299	helix
Ac-A_{15}HGH-NH_2 + $2H^+$	339	332	helix
Ac-$A_{15}H$ + H^+	299	305	helix

[a] Cross sections determined at 300 K. [b] Cross section calculated for the lowest energy conformation found in the MD simulations.

water adsorption is observed for helical Ac-A_{20}K+$2H^+$, though the helix adsorbs only a single water molecule. Van't Hoff plots for the two doubly charged peptides are shown in Figure 3. Analysis of the van't Hoff plots yields $\Delta H° = -47.7$ kJ mol^{-1} and $\Delta S° = -92$ J K^{-1} mol^{-1} for globular $AcKA_{20}$+$2H^+$ and $\Delta H° = -40.6$ kJ mol^{-1} and $\Delta S° = -87$ J K^{-1} mol^{-1} for helical AcA_{20}K+$2H^+$, respectively. These results are compared in Table 1 to the other values obtained in this work.

Shorter peptides were studied to see how the length affected the thermodynamics for adsorption of the first water molecule. Cross sections measured for Ac-KA_{15}+H^+, Ac-A_{15}K+H^+, and Ac-A_{15}K+$2H^+$ are summarized in Table 2. Comparison with the cross sections for the singly charged analogues and with the results of molecular dynamics simulations (see below) indicate that Ac-A_{15}K+$2H^+$ is helical. Hydration studies were not performed for Ac-KA_{15}+$2H^+$ because of the presence of a significant amount of (Ac-KA_{15}+$2H^+$)$_2$ dimer which survived both at high capillary temperature and at high injection energy. The helical Ac-A_{15}K+H^+ peptide showed no water adsorption. However, both globular Ac-KA_{15}+H^+ and helical Ac-A_{15}K+$2H^+$ adsorbed water. The van't Hoff plots were of similar quality to those shown in Figure 3. The van't Hoff plots provided $\Delta H° = -48.9$ kJ mol^{-1} and $\Delta S° = -131$ J K^{-1} mol^{-1} for globular $AcKA_{15}$+H^+ and $\Delta H° = -47.6$ kJ mol^{-1} and $\Delta S° = -114$ J K^{-1} mol^{-1} for helical AcA_{15}K+$2H^+$, respectively. These values are compared to the others obtained in this work in Table 1.

Although the doubly charged helices do adsorb water, we attempted to design helices that might adsorb water more

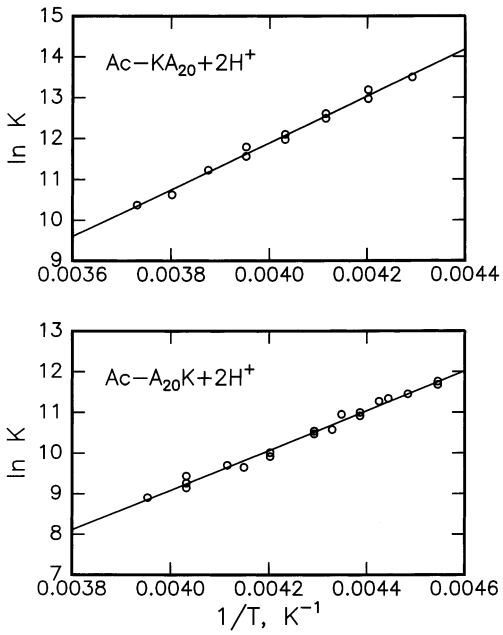

Figure 3. Van't Hoff plots (ln K against $1/T$) for the addition of the first water molecule to Ac-KA_{20}+$2H^+$ and Ac-$A_{20}K$+$2H^+$. The points are the measurements, and the lines are linear least-squares fits.

strongly. Our first attempt was Ac-A_{15}HGH-NH_2, where we hoped that a water molecule would become bound between the two histidines. Our original intent was to study the singly charged peptide; however, this is not generated in significant abundance. The main peak in the mass spectrum of this peptide is the doubly charged ion, Ac-A_{15}HGH-NH_2+$2H^+$. The cross section determined for Ac-A_{15}HGH-NH_2+$2H^+$ is given in Table 2. Comparison with molecular dynamics simulations (see below) indicates that Ac-A_{15}HGH-NH_2+$2H^+$ is predominantly helical. The helical Ac-A_{15}HGH-NH_2+$2H^+$ peptide was found to adsorb water very strongly. Water adsorption was detectable at a significantly higher temperature than for the other helical peptides discussed above. $\Delta H°$ and $\Delta S°$ were found to be significantly larger as well ($\Delta H° = -59.9$ kJ mol^{-1} and $\Delta S° = -162$ J K^{-1} mol^{-1}). Ac-A_{15}H was synthesized for comparison with the Ac-A_{15}HGH-NH_2 peptide and in an effort to make a singly charged helix that might adsorb water more strongly. The singly charged ion was prominent in the mass spectrum for Ac-A_{15}H. Mobility measurements and molecular dynamics simulations (see below) indicate that the Ac-A_{15}H+H^+ peptide is also helical (see Table 2). The helical Ac-A_{15}H+H^+ peptide was found to adsorb water even more strongly than Ac-A_{15}HGH-NH_2+$2H^+$. The values $\Delta H° = -62.7$ kJ mol^{-1} and $\Delta S° = -187$ J K^{-1} mol^{-1} were deduced from the van't Hoff plot for addition of the first water molecule to Ac-A_{15}H+H^+. These are the largest values of $\Delta H°$ and $\Delta S°$ found in these studies for either helices or globules, singly or doubly charged (see Table 1).

The drift time distributions measured for Ac-A_{15}H+H^+ at low temperature show two poorly resolved features. For all the other peptides studied here, single features were observed for all temperatures (excluding features assigned to dimers and other multimers). Two features were observed at low temperature for both Ac-A_{15}H+H^+ and Ac-A_{15}H+H^++H_2O (the peptide with a single water molecule attached). However, the relative abundances of the two peaks are not exactly the same for Ac-A_{15}H+H^+ and Ac-A_{15}H+H^++H_2O. The most likely interpretation of this result is that there are two conformations (which do not interconvert on the experimental time scale) that have slightly different propensities to adsorb water. The emergence of the two conformations at low temperature does not appear to affect the van't Hoff plot for the addition of the first water to Ac-A_{15}H+H^+. The van't Hoff plot remains linear over the entire temperature range examined, with $R^2 = 0.99$. The difference between the cross sections for the two conformations found at low temperature is relatively small (313 and 321 A^2 at 225 K); it may result from a difference in the arrangement of the imidazole side chain of histidine, though the precise cause is difficult to pinpoint with certainty.

The drift time distributions for the other peptides studied here are usually narrow and close to the width expected for a single conformation. The only exception is Ac-KA_{20}+$2H^+$, for which the measured peak is slightly broader than that expected for a single component. This indicates that there are at least two, and maybe more, slightly different globular conformations present for Ac-KA_{20}+$2H^+$. These different conformations may have slightly different propensities to adsorb water, in which case the values for $\Delta H°$ and $\Delta S°$ we deduce from the van't Hoff plots are averages. Even when the drift time distribution appears narrow, there may be more than one conformation present. So different conformations with slightly different propensities to adsorb water may occur for some of the other peptides studied here as well.

Molecular Dynamics Simulations: Methods

We have performed molecular dynamics (MD) simulations to obtain trial conformations for comparison with the measured cross sections and to obtain some insight into the results of the rehydration studies. Since the simulations employ an empirical force field, we can only hope to use them to provide insight into the gross features of the experimental results, such as why different peptides adsorb water strongly, weakly, or not at all. The minor differences predicted by the simulations may not be reliable.[46] The use of more sophisticated methods is precluded by the size of the peptides studied here. All calculations were performed with the MACSIMUS suite of programs[47] using the CHARMM 21.3 parameter set. The first objective is to generate low-energy conformations for the peptides. Most of these simulations were done using a new simulated annealing schedule designed to prevent trapping in high-energy local minima.[48] The new schedule routinely generates helices starting from a linear structure (with a helix-forming peptide). However, helical target structures were started from an ideal α-helix, while globular target structures were started from a linear structure. At least 10 simulated annealing runs were performed for each peptide.

The interaction between the peptides and water was examined by taking the lowest energy structure generated in the simulated annealing runs and introducing a TIP3P water near the α-carbon of each residue in turn. For each residue, a 240 ps MD simulation was performed (during which time the water can be

(46) Mitchell, J. B. O.; Price, S. L. *Chem. Phys. Lett.* **1991**, *180*, 517−523.
(47) http://www.icpf.cas.cz/jiri/macsimus/default.htm
(48) Following 15 ps at 600 K, the temperature is stepped down by 10 K for 45 ps. The temperature is then stepped up by 200 K for 15 ps, and stepped down by 210 K for 45 ps. This 200 K step-up and 210 K step-down cycle is repeated until the temperature reaches 530 K. The temperature is then dropped to 300 K for 45 ps, raised to 500 K for 15 ps, and then the schedule terminates with 360 ps at 253 K. The total elapsed time is 915 ps.

quite mobile until it finds a favorable binding site); the water was then removed, and another 15 ps MD simulation was run. The water-binding energy (which we assume is equivalent to the negative of the enthalpy change for hydration) is then approximated by the difference in the average potential energies taken from the end of the simulations with and without the water (the water by itself contributes less than 1 kJ mol^{-1}). Addition of water often caused subtle conformational changes, but for a few simulations drastic changes occurred (often with ~10% change in the cross section), and these were discarded (the criteria used was >5% change in the calculated cross section). The experimental results indicate there are no substantial conformational changes with water addition.

The ion mobility measurements provide average collision cross sections (or more correctly, average collision integrals) for the peptides. Average collision integrals can be calculated for the conformations obtained in the MD simulations for comparison with the experimental results. In the present work, the collision integrals were calculated using an empirical correction[49] to the exact hard-spheres scattering model,[50] averaging over 50 snapshots taken from the MD simulations over 35 ps. In the exact hard-spheres scattering model, the peptide ion is treated as a collection of hard spheres, and the interactions between the buffer gas atom and the peptide ion are treated as hard-sphere interactions. The collision integral is obtained by averaging a function of the scattering angle over impact parameter and collision geometry. The scattering angle is the angle between the incoming and outgoing trajectories in a collision between a buffer gas atom and the peptide ion. It is important that the scattering process is treated correctly; the geometric cross section is a poor approximation for large molecules.[51] Comparison with trajectory calculations has shown that the exact hard-spheres scattering model overestimates the cross sections slightly, and so an empirical correction was introduced.[49] If the conformation is correct, the calculated cross section is expected to be within 2% of the experimental value.[51] In the calculations, we assume that there is no preferred collision geometry; in other words, there is no alignment in the drift field. This assumption is valid in the low-field regime where the measurements were performed. In this regime, the motion of the ions in the drift field can be thought of as directed diffusion.

Molecular Dynamics Simulations: Results

Water Adsorption on Globular Ac-KA_{20}+H^+ and Helical Ac-$A_{20}K$+H^+. For these peptides, we assume that the lysine side chain is protonated. For Ac-KA_{20}+H^+, the charge is at the N-terminus, where unfavorable interactions with the helix macrodipole destabilize the helix. The lowest energy conformation found in the simulations is a globule, which is shown in Figure 4a. This and the following figures show a snapshot of the conformation taken at the end of the MD run. The conformation shown in Figure 4a has a loop region and a short helical section stabilized by the lysine side chain wrapping around and interacting with the C-terminal end. The calculated cross section for this conformation matches the measured value (see Table 2). For Ac-A_{20}K+H^+, the charge is at the C-terminus, where it interacts favorably with the helix macrodipole. The lowest energy conformation found in the simulations is an α-helix, where the lysine side chain loops around and the protonated amine hydrogen bonds to the dangling CO groups at the C-terminal end of the helix. The calculated cross section for this conformation is in good agreement with the measured value (see Table 2).

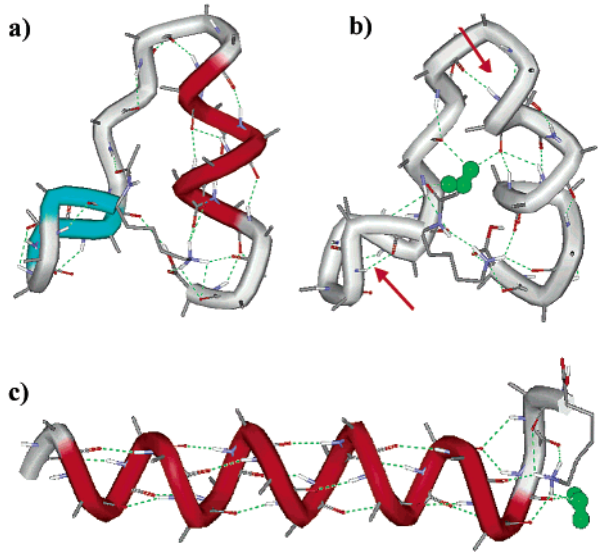

Figure 4. Conformations for helical Ac-A_{20}K+H^+ and globular Ac-KA_{20}+H^+. (a) The lowest energy conformation found in the simulations for globular Ac-KA_{20}+H^+. (b) The arrangement with the highest water-binding energy for globular Ac-KA_{20}+H^+. (c) The arrangement with the highest water-binding energy for helical Ac-A_{20}K+H^+. The images were generated with the Weblab Viewer (MSI Inc, San Diego, CA). α-Helical regions are red; β-sheet regions are blue. Hydrogen bonds (based on a distance criteria of <2.5 Å) are indicated by dashed green lines. The water is represented by a collection of three green spheres. The red arrows in (b) show the water-binding pockets discussed in the text.

Substantial differences in water affinities were observed experimentally for these two peptides. The arrangements with the highest water-binding energies found in the simulations for globular Ac-KA_{20}+H^+ and helical Ac-A_{20}K+H^+ are shown in Figure 4b and c, respectively. In the simulations for the Ac-KA_{20}+H^+ globule, it was found that water preferred to bind in pocket-like sites (folds in the peptide surface where multiple hydrogen-bonding partners are available). There are three preferred pocket-like sites in the globular conformation shown in Figure 4: near the turn region from Lys1 to Ala6 (marked by the lower red arrow in the figure), at the end of the short helical section from around Ala11 to Ala14 (marked by the upper red arrow in the figure), and between the side of the helix and the loop section (which is occupied by a water molecule in the figure). In this site, the water is involved in an expansive network of hydrogen bonds involving the acetyl carbonyl group and the carbonyl groups of Ala14 and Ala9. Water adsorption near the charged group is less favorable because the charged primary amine interacts very strongly with the backbone carbonyls, and these interactions must be disrupted before the water can bind.[45,52] In the MD simulations, the water molecule is initially quite mobile and moves around until it finds a favorable binding site, which is usually one of the three

(49) Kinnear, B. S.; Kaleta, D. T.; Kohtani, M.; Hudgins, R. R.; Jarrold, M. F. *J. Am. Chem. Soc.* **2000**, *122*, 9243−9256.
(50) Shvartsburg, A. A.; Jarrold, M. F. *Chem. Phys. Lett.* **1996**, *261*, 86−91.
(51) Shvartsburg, A. A.; Schatz, G. C.; Jarrold, M. F. *J. Chem. Phys.* **1998**, *108*, 2416−2423.
(52) Mao, Y.; Ratner, M. A.; Jarrold, M. F. *J. Am. Chem. Soc.* **2000**, *122*, 2950−2951.

mentioned above. It usually takes less than 100 ps for the water to become localized.

The interaction between water and the Ac-$A_{20}K+H^+$ helix is much weaker than for the globule. Any water molecule placed in the middle region of the helix either desorbed or migrated to one of the ends, where hydrogen-bonding partners are available. The C-terminus appears to be preferred, presumably because the charge there provides some additional electrostatic stabilization. In the conformation shown in Figure 4, the water molecule has penetrated between a carbonyl CO group and the charged amine to form hydrogen bonds to both of them. Even though the charge is less well shielded than in the globule, this is still not a strongly favored process, and the water-binding energy remains relatively low. The water is bound less strongly to the helix than to the globule because it is unable to participate in an extended hydrogen-bonding network. This is due to the fact that the hydrogen-bonding network of the helix ties up a large fraction of the potential hydrogen-bonding partners.

The highest water-binding energies found in the simulations are 52 kJ mol^{-1} for globular Ac-$KA_{20}+H^+$ and 43 kJ mol^{-1} for helical Ac-$A_{20}K+H^+$. Assuming that the $\Delta S°$ values for addition of the first water molecule to the helix and globule are equal, the difference in the binding energy predicted by the simulations (9 kJ mol^{-1}) is just enough to account for the absence of a measurable helix−water adduct. TIP3P uses average properties appropriate for the liquid state,[53] and the dipole moment, in particular, is too large (2.347 D), which will exaggerate charge−dipole and dipole−dipole interactions. Thus the interaction between the water molecule and the helix may be slightly overestimated.

The Doubly Charged Species: Ac-$KA_{20}+2H^+$ and Ac-$A_{20}K+2H^+$. The location of the second charge is an issue for the doubly charged peptides. While it is clear that the charge should reside on an amide CO, there are 21 different sites available. The proton may even be mobile, jumping among the different sites.[54,55] However, at the temperatures employed here, the charge is probably localized (or at least moves very slowly) because of the activation barrier associated with disrupting and re-forming the shell of carbonyl groups that stabilizes it. In any case, the possibility of a mobile proton is not incorporated into the MD simulations. Placing the second charge at the C-terminus of Ac-$KA_{20}+2H^+$ resulted in an unraveled α-helix with a large collision cross section. Protonation of the amide CO at the middle (Ala11) led to globular conformations. As shown in Table 2, the cross section for the lowest energy globule obtained in this way is in good agreement with the measured value. Protonation at other sites may also lead to globular conformations, some of which may be lower in energy than the one obtained by protonating Ala11.

Eight different protonation sites were tried for the second proton in Ac-$A_{20}K+2H^+$. While the force field energies for chemically different species are usually not comparable, in the present case the difference is only the location of a chemically identical protonation site, and so a reasonable comparison can be made. For Ac-$A_{20}K+2H^+$, the low-energy conformations

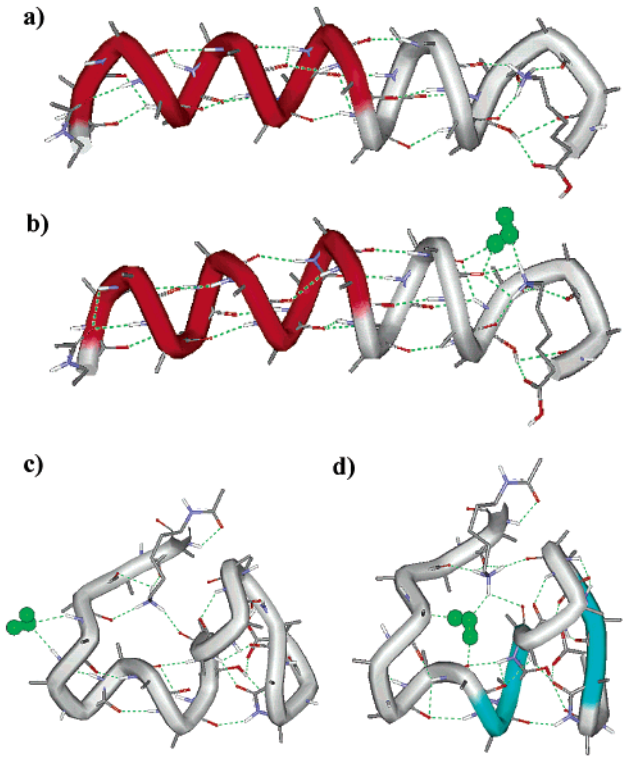

Figure 5. Conformations for helical Ac-$A_{20}K+2H^+$ and globular Ac-$KA_{20}+2H^+$. (a) The lowest energy conformation found in the simulations for helical Ac-$A_{20}K+2H^+$. (b) The arrangement with the highest water-binding energy for helical Ac-$A_{20}K+2H^+$. (c,d) The arrangements with the highest water-binding energies for globular Ac-$KA_{20}+2H^+$. The two arrangements shown have almost identical water-binding energies. The images were generated with the Weblab Viewer (MSI Inc, San Diego, CA). α-Helical regions are red; β-sheet regions are blue. Hydrogen bonds (based on a distance criteria of <2.5 Å) are indicated by dashed green lines. The water is represented by a collection of three green spheres.

were obtained by placing the second proton near the C-terminus. This led to the formation of partial π-helices (π-helix at the C-terminus and α-helix at the N-terminus). A π-helix has $i,i+5$ hydrogen bonds (4.4 residues per turn), while an α-helix has $i,i+4$ hydrogen bonds (3.6 residues per turn). The lowest energy Ac-$A_{20}K+2H^+$ helix generated in the simulations is shown in Figure 5a. This was obtained by protonating the carbonyl CO of Ala17. In this, and in many other low-energy helices found in the Ac-$A_{20}K+2H^+$ simulations, the charges are quite close together (within 4 Å). Favorable interactions between the helix macrodipole and the two charges presumably compensate for their mutual repulsion. Similar cooperative stabilizing effects have been discussed in the context of noncovalent complexes of unsolvated peptides.[56] The presence of the two charges causes quite extensive disruption of the C-terminal end of the helix (the lysine side chain now appears to be inserted into the last helix turn), presumably in order to maximize the shielding of the charge. The calculated cross section for the lowest energy Ac-$A_{20}K+2H^+$ helix found in the simulations is significantly smaller than the measured value (see Table 2). The small cross section presumably results from the partial π-helical character and from the relatively compact arrangement at the C-terminal end.

(53) Lyne, P. D.; Hodoscek, M.; Karplus, M. *J. Phys. Chem. A* **1999,** *103*, 3462−3471.
(54) Dongre, A. R.; Jones, J. L.; Somogyi, Á.; Wysocki, V. H. *J. Am. Chem. Soc.* **1996**, *118*, 8365−8374.
(55) Rodriquez, C. F.; Cunje, A.; Shoeib, T.; Chu, I. K.; Hopkinson, A. C.; Siu, K. W. M. *J. Am. Chem. Soc.* **2001**, *123*, 3006−3012.
(56) Kaleta, D. T.; Jarrold, M. F. *J. Am. Chem. Soc.* **2002**, *124*, 1154−1155.

Table 3. Table of Some Related Water Adsorption Thermochemistry Values Taken from Previous Work

species	measured $\Delta H°$, kJ mol^{-1}	measured $\Delta S°$, J K^{-1} mol^{-1}
NH_4^+ [a]	−86.2	−103
$CH_3NH_3^+$ [b]	−70.3	−90.1
$C_2H_5NH_3^+$ [c]	−73.2	−108
n-$C_6H_{13}NH_3^+$ [d]	−63.6	−95.4
$HCONH_3^+$ [b]	−88.7	−114
$(CH_3)_2COH^+$ [b]	−85.8	−109
$NH_3^+(CH_2)_6NH_3^+$ [d]	−74.5	−87.9
$NH_3^+(CH_2)_{12}NH_3^+$ [d]	−65.7	−85.0
imidazole-H^+ [e]	−61.9	−99.6
CH_3COH^+-Ala-OCH_3 [f]	−54.4	−88.7

[a] Reference 33. [b] Reference 32. [c] Reference 31. [d] Reference 36. [e] Reference 35. [f] Reference 37.

Water binds only to the ends of the Ac-$A_{20}K+2H^+$ helix in the simulations; it prefers the charged C-terminus. The arrangement with the highest water-binding energy found in the simulations is shown in Figure 5b. In this arrangement, the water interacts with the protonated amine and two backbone CO groups. Comparison of parts a and b of Figure 5 shows water-binding to the protonated amine without disrupting other interactions (unlike the singly charged helix, where formation of a hydrogen bond to water required the disruption of another to a backbone CO). This explains why the doubly charged helix has a larger propensity to adsorb water than the singly charged one (see Table 1). The water is able to bind to the protonated amine without disrupting other interactions because the two charges are so close in the doubly charged helix that they are not as well shielded.

Previous work has shown that water binds more strongly to an unshielded protonated carbonyl group than to an unshielded $-NH_3^+$ group (compare the hydration thermodynamics for $(CH_3)_2COH^+$ and $C_2H_5NH_3^+$ given in Table 3), yet in the structure shown in Figure 5b, the water is bound to the amine rather than the carbonyl group. One contributing factor may be that the amide carbonyl is more basic (better able to stabilize the positive charge) than a ketone carbonyl, and more like an amine in its basicity.[55] But probably more important is the fact that the water interacts with more than just the protonated group. In Figure 5b, the water also hydrogen-bonds to two carbonyl groups, in addition to the $-NH_3^+$ group. The energetic cost of disrupting existing hydrogen bonds (while not a factor here) will also contribute to the overall energetics of water binding. The $-NH_3^+$ group seems to make more but weaker hydrogen bonds than the protonated carbonyl group.

When a water molecule interacts with globular Ac-$KA_{20}+2H^+$, it localizes in a few favorable binding sites, much like the singly charged peptide. The two arrangements with the largest water-binding energies found for the lowest energy Ac-$KA_{20}+2H^+$ conformation are shown in Figure 5c and d. The water-binding energies for these two arrangements are almost identical. In Figure 5c, the water is bound on the outside of the peptide by two hydrogen bonds to backbone NH groups. In Figure 5d, the water is inserted into a hydrogen bond between a backbone CO and the protonated amine and forms another hydrogen bond to another backbone CO. These two conformations illustrate that the energetics for binding a water molecule in a pocket and on the outside can be quite close for the doubly charged globule. With two charges to shield, the doubly charged globule is a tight-knit system of hydrogen bonds with less flexibility than the singly charged analogue. Binding a water molecule inside a pocket requires a significant reorganization to make room for it. In Figure 5d, for example, it is necessary to disrupt some hydrogen bonds in order to get the water to fit. Binding water on the outside should minimize the perturbation to the geometry. The most favorable situation would be to have multiple hydrogen-bonding partners already in the perfect orientation to bind a water molecule (then there is no energetic penalty associated with rearranging the peptide).

Length Effects: Ac-$KA_{15}+H^+$, Ac-$A_{15}K+H^+$, and Ac-$A_{15}K+2H^+$. Calculated cross sections for the lowest energy structures found in the MD simulations are compared to the measured values for Ac-$KA_{15}+H^+$, Ac-$A_{15}K+H^+$, and Ac-$A_{15}K+2H^+$ in Table 2. There is good agreement for all species, even for the doubly charged helix, which is again a partial π-helix (though with a less compact arrangement at the C-terminus than for Ac-$A_{20}K+2H^+$).

The lowest energy conformation found for globular Ac-$KA_{15}+H^+$ has some features in common with that for Ac-$KA_{20}+H^+$, in particular a short helical section stabilized by the lysine side chain wrapped around to the C-terminal end. The preferred water-binding sites are close to the N-terminal end of the short helical section and near the charge. The site near the charge appears to have the highest water-binding energy. Here, the water forms a hydrogen bond to the protonated amine without displacing a CO group. This presumably occurs because the charge is less well shielded in Ac-$KA_{15}+H^+$ than in Ac-$KA_{20}+H^+$, because fewer backbone CO groups are available. This provides an explanation for why Ac-$KA_{15}+H^+$ has a more negative $\Delta H°$ than Ac-$KA_{20}+H^+$, though the difference in the simulations is substantially larger than the experimental result (see Table 1). In the most favorable water-binding site for helical Ac-$A_{15}K+H^+$, the water disrupts hydrogen bonds between the protonated amine and a backbone CO and forms two hydrogen bonds between water and the protonated amine and one hydrogen bond between the water and the backbone CO. The water-binding energy for helical Ac-$A_{15}K+H^+$ is substantially less than that for globular Ac-$KA_{15}+H^+$, which explains why no hydration product is observed for the helix. The measured $\Delta H°$ is significantly larger for Ac-$A_{15}K+2H^+$ than for Ac-$A_{20}K+2H^+$. This difference is only partly reflected in the simulations where the enhanced water-binding energy for Ac-$A_{15}K+2H^+$ appears to result, principally because the second charge (which is located near the C-terminus on the CO of Ala14 in the lowest energy conformation found in the simulations) is very poorly shielded. It is possible that the more extensive disruption of the C-terminal end that occurs for Ac-$A_{20}K+2H^+$ (and presumably leads to better shielding) is unfavorable in a shorter helix.

Peptides Designed To Bind Water: Ac-A_{15}HGH-NH_2+2H^+ and Ac-$A_{15}H+H^+$. For both peptides, we assumed that the histidine side chains are protonated. And for both peptides, the lowest energy conformations found in the simulations were helical, with calculated cross sections in reasonable agreement with the measured values (see Table 2). The lowest energy conformation found for Ac-$A_{15}HGHNH_2$-$2H^+$ is shown in Figure 6a. The two protonated histidines disrupt the C-terminal end of the helix, so that it is not α-helical over its whole length. When histidine is protonated, the charge is distributed over both

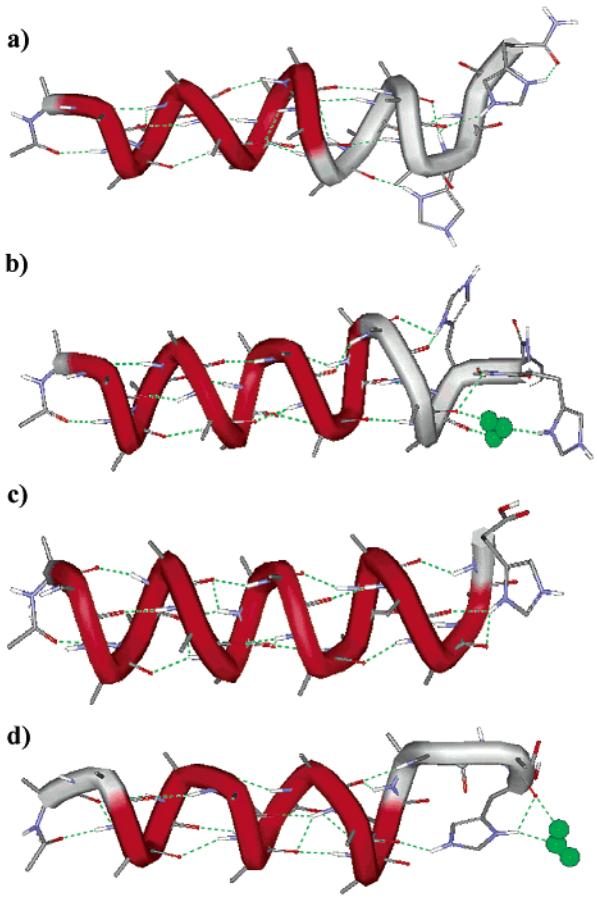

Figure 6. Conformations for helical Ac-$A_{15}HGH+2H^+$ and helical Ac-$A_{15}H+H^+$. (a) The lowest energy conformation found in the simulations for Ac-$A_{15}HGH+2H^+$. (b) The highest binding energy site found by manipulating Ac-$A_{15}HGH+2H^+$. (c) The lowest energy conformation found in the simulations for Ac-$A_{15}H+H^+$. (d) The highest binding energy site found by manipulating Ac-$A_{15}H+H^+$. The images were generated with the Weblab Viewer (MSI Inc, San Diego, CA). α-Helical regions are red; β-sheet regions are blue. Hydrogen bonds (based on a distance criteria of <2.5 Å) are indicated by dashed green lines. The water is represented by a collection of three green spheres.

secondary amines in the ring. It is clearly more difficult to shield the bulky charged histidine, and in the conformation shown in Figure 6a, one of the secondary amines is completely unshielded, unlike the lysine analogue. Not surprisingly, this is the highest binding energy site for a water molecule, but the binding energy was found to be only 51 kJ mol^{-1} (largest from 36 MD runs). This is larger than the binding energies to the singly charged Ac-$A_{15}K+H^+$ and Ac-$A_{20}K+H^+$ helices and comparable to the binding energies determined for the doubly charged Ac-$A_{15}K+2H^+$ and Ac-$A_{20}K+2H^+$ helices, but it is significantly smaller than expected from the experimental results. This disagreement may indicate that a significant structural rearrangement occurs when the water is adsorbed, so that a network of hydrogen bonds can be established. By manipulating the Ac-$A_{15}HGH$-NH_2+2H^+ peptide so that a water molecule is placed between the imidazole side chain of a histidine and a carbonyl, we found one binding site with a significantly higher binding energy. This site, shown in Figure 6b, has the water hydrogen-bonded to one histidine and two carbonyl CO groups. The binding energy is 71 kJ mol^{-1}, which provides reasonable agreement with the measured value.

The lowest energy conformation found for Ac-$A_{15}H+H^+$ is α-helical, with the protonated histidine sitting over the C-terminus (see Figure 6c). Because of the geometry and size of the histidine side chain, only one of the charged secondary amines can interact with dangling CO groups at the end of the helix, leaving the other completely unshielded. The unshielded secondary amine is the favored binding site of water, according to the simulations. However, the binding energy is only 53 kJ mol^{-1}, which is less than the experiments suggest (Ac-$A_{15}H+H^+$ has the largest $\Delta H°$ of the peptides studied here). This suggests that the water may be bound more strongly to Ac-$A_{15}H+H^+$ in a way analogous to that shown in Figure 6b for Ac-$A_{15}HGH$-NH_2+2H^+, where the water is trapped between the histidine side chain and the end of the helix. However, the water invariably escaped from this site when MD simulations for Ac-$A_{15}H+H^+$ were started from a similar geometry. The resulting conformation with the highest water-binding energy (61 kJ mol^{-1}) is shown in Figure 6c. Here the water is in a bridging position between a backbone CO and the histidine side chain. The water-binding energy for this conformation is still relatively low.

Discussion

Comparison with Thermochemistry for the Hydration of Small Protonated Molecules. Table 3 shows $\Delta H°$ and $\Delta S°$ for the adsorption of the first water molecule onto a selection of small protonated molecules that are related to the peptides studied here. The enthalpy changes are generally larger for the smaller molecules in Table 3 than for the peptides, because the small molecules have exposed charges, except for CH_3COH^+-Ala-OCH_3, where the charge is probably partially shielded by the backbone carbonyl on the alanine. The $\Delta H°$ for CH_3COH^+-Ala-OCH_3 is the smallest in Table 3, though it is larger than for all the peptides studied here, except for those containing a histidine. The entropy changes shown in Table 3 are less variable, and on average smaller, than the entropy changes determined for the peptides. This may reflect the simpler nature of the interactions between the water and the unshielded charges in the small protonated molecules.

Insight from the MD Simulations. We cannot expect good quantitative agreement between the results of the simulations and the experiments because of the shortcomings associated with the use of an empirical force field. However, the simulations often reproduced the main features of the experimental results. Thus, they provide useful insight into the factors that are important in the adsorption of a water molecule onto a peptide, and how this process is affected by conformation, charge, and composition.

The MD simulations show that large water-binding energies are achieved by establishing a network of hydrogen bonds to different sites on the peptide. This is facilitated in pocket-like sites either on the surface or within the peptide. Unless the charge is poorly shielded, the charged sites do not emerge as particularly favorable sites for hydration because interaction with water requires disruption of other interactions, primarily with backbone CO groups. This observation is supported by the experimental measurements; the magnitude of the measured enthalpy changes is consistent with the formation of several hydrogen bonds to neutral species rather than the larger enthalpy change expected for interaction with an unshielded charge. Many

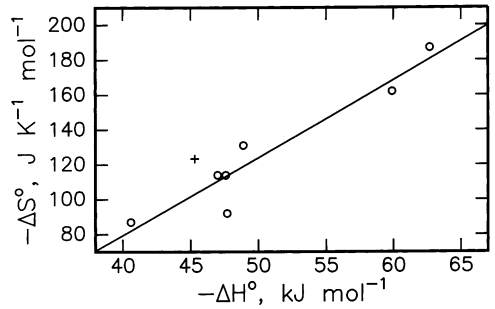

Figure 7. Plot of $\Delta S°$ against $\Delta H°$ for the addition of a water molecule to the peptides studied here. The open circles are the experimental data, and the line is a least-squares fit. The cross shows $\Delta S°$ and $\Delta H°$ for adsorbing a vapor-phase water molecule onto liquid water.

of the variations in the enthalpy change with charge, conformation, and composition can be rationalized in terms of changes in how well the charge is shielded. Water generally binds more strongly to doubly charged peptides because the extra charge disrupts the shielding. The shielding seems to be less effective for smaller peptides because they have fewer hydrogen-bonding partners. And finally, water binds more strongly to histidine-containing helical peptides, at least partly because of poor shielding of the sterically cumbersome histidine side chain.

The Entropy Change for Addition of a Water Molecule in the Vapor Phase. While the MD simulations provide some insight into the factors that affect the enthalpy change associated with binding the water molecule, they provide no real information about what is important in determining the entropy change. The entropy change can be broken down as follows:

$$\Delta S° = \Delta S_{vib} + S^{complex}_{vib/rot} - S^{water}_{trans} - S^{water}_{rot} \qquad (4)$$

where ΔS^{water}_{trans} and ΔS^{water}_{rot} are the translational and rotational entropy of the water molecule that are lost when water binds to the peptide, $\Delta S^{complex}_{vib/rot}$ is the entropy associated with the six new internal degrees of freedom (vibrations and internal rotations) that are formed when the water binds, and ΔS_{vib} is the change in the vibrational entropy of the peptide when the water binds,

$$\Delta S_{vib} = S^{peptide\ in\ complex}_{vib} - S^{peptide}_{vib} \qquad (5)$$

This is negative if the water molecule stiffens-up the peptide, and positive if the water molecule loosens-up the peptide. ΔS^{water}_{trans} and ΔS^{water}_{rot} are easily calculated using the standard methods of statistical thermodynamics,[57] from which we find $\Delta S^{water}_{trans} + \Delta S^{water}_{rot} = 185.6$ J K^{-1} mol^{-1}. If $\Delta S_{vib} = 0$, then the overall $\Delta S°$ can, in principle, range from a slightly positive value to -185.6 J K^{-1} mol^{-1}, depending on the size of $\Delta S^{complex}_{vib/rot}$. If the water is strongly bound to the peptide, then the new modes generated when the water binds are expected to have high frequencies, while if the water is weakly bound, the new modes should have low frequency. Thus, a correlation between the entropy change and enthalpy change is expected for binding a water molecule. Figure 7 shows a plot of $\Delta S°$ against $\Delta H°$ for the addition of a water molecule to the peptides studied here. The open circles are the experimental data, and the line is a least-squares fit. There is clearly a correlation between $\Delta S°$ and $\Delta H°$, with $R^2 = 0.909$, although there is no real reason to expect the correlation to be linear. The correlation indicates that the relationship between the stiffness of the new vibrational modes and the binding energy is a factor in determining the size of the entropy change. However, it is not the only factor, because the correlation is not perfect. The point due to globular Ac-KA_{20}+2H$^+$ ($\Delta H° = -47.7$ kJ mol^{-1} and $\Delta S° = -92$ J K^{-1} mol^{-1}) clearly has a low value for $\Delta S°$, suggesting that ΔS_{vib} is positive and that water adsorption loosens-up this peptide. On the other hand, the entropy change for water adsorption on helical Ac-A_{15}H+H$^+$ ($\Delta S° = -187$ J K^{-1} mol^{-1}) is too negative to be accounted for without invoking a negative value for ΔS_{vib}, indicating that water adsorption stiffens-up the peptide in this case. This may also be true for Ac-A_{15}HGH$-$NH$_2$+2H$^+$ as well, because this peptide also has a large value for the entropy change. Comparison of the large entropy changes of the histidine-containing peptides (-187 J K^{-1} mol^{-1} for Ac-A_{15}H+H$^+$) to the moderate entropy change for protonated imidazole (-99.6 J K^{-1} mol^{-1} in Table 3) also indicates that water adsorption on the peptides causes a stiffening or the introduction of some sort of constraint.

A useful benchmark for comparison with the experimental results is $\Delta H°$ and $\Delta S°$ for adsorption of a vapor-phase water molecule onto liquid water ($\Delta H° = -45.3$ kJ mol^{-1} and $\Delta S° = -123$ J K^{-1} mol^{-1}). This value is represented by the cross in Figure 7. The enthalpy and entropy changes for binding a water molecule to the peptides are close to $\Delta H°$ and $\Delta S°$ for adsorbing a vapor-phase water molecule onto liquid water. This indicates that $\Delta H°$ and $\Delta S°$ for transferring a water molecule from the liquid to the solvation shell of the peptide are small, even for the first water molecule. All of the peptides except for Ac-A_{15}HGH-NH$_2$ and Ac-A_{15}H+H$^+$ are insoluble in water. Even these peptides were found to absorb a maximum of only three water molecules under the conditions we employed. The second water molecule is significantly less strongly bound than the first for all the peptides studied here. We were not able to obtain reliable experimental data for the adsorption of the second and subsequent water molecules.

Interaction between Water and the Helices. In *all* of the MD simulations conducted on α-helical peptides, lasting interactions between water and the amide groups involved in the network of hydrogen bonds that form the helix were never observed. The water is weakly bound to the side of the helix due to the unfavorable hydrogen-bonding geometry and its inability to form a network of hydrogen bonds. The failure to observe any hydration of the Ac-A_{20}K+H$^+$ helix places an upper limit on the free energy for interaction of water with the helical peptide group of > -10 kJ mol^{-1} at 243 K (see Table 1). Even though the hydration of this group is not favorable, it has been argued that its hydration is an important factor in driving helix formation[58] and determining helix propensities.[59−62] Previous MD studies of the interaction of water with helices have examined how the water destabilizes the helix[63,64] and how water

(57) McQuarrie, D. A. *Statistical Mechanics*; Harper & Row: New York, 1976.
(58) Avbelj, F.; Luo, P.; Baldwin, R. L. *Proc. Natl. Acad. Sci. U.S.A.* **2000**, *97*, 10786−10791.
(59) Avbelj, F.; Moult, J. *Biochemistry* **1995**, *34*, 755−764.
(60) Avbelj, F.; Fele, L. *J. Mol. Biol.* **1998**, *279*, 665−684.
(61) Avbelj, F. *J. Mol. Biol.* **2000**, *300*, 1335−1359.
(62) Luo, P.; Baldwin, R. L. *Proc. Natl. Acad. Sci. U.S.A.* **1999**, *96*, 4930−4935.
(63) DiCapua, F. M.; Swaminathan, S.; Beveridge, D. L. *J. Am. Chem. Soc.* **1990**, *112*, 6768−6771.
(64) Soman, K. V.; Karimi, A.; Case, D. A. *Biopolymers* **1991**, *31*, 1351−1361.

insertion can induce the helix to bend.[65] No evidence for this behavior was found in our simulations, possibly because the water molecules became localized at the end of the helices.

Conclusions

Water adsorption on a variety of unsolvated alanine-based peptides has been studied using equilibrium measurements and molecular dynamics simulations. Globular Ac-KA_n+H^+ peptides were found to adsorb water, while no water adsorption was detected for helical Ac-A_nK+H^+. MD simulations suggest that it is necessary to establish a network of hydrogen bonds involving several different hydrogen-bonding partners in order to achieve strong interactions between the water molecule and the peptide. For geometric reasons, it is not possible to establish such a network with the Ac-A_nK+H^+ helices. When the charge is well shielded by interactions with backbone CO groups, it is often not directly involved in adsorption of the water molecule, because it is necessary to disrupt the existing interactions in order to make room for the water. However, for multiply charged peptides and for peptides that incorporate histidine instead of lysine, the shielding is less effective, and the charge site is often involved. Of the peptides that were examined, those that incorporate histidine have the strongest interactions with water.

Acknowledgment. We thank Jiri Kolafa for use of his MACSIMUS molecular modeling programs and for his helpful advice. We gratefully acknowledge the support of the National Institutes of Health.

JA012755R

(65) DiCapua, F. M.; Swaminathan, S.; Beveridge, D. L. *J. Am. Chem. Soc.* **1991**, *113*, 6145−6155.